Subcapsular encounter and complement-dependent transport of immune complexes by lymph node B cells

Tri Giang Phan[1], Irina Grigorova[1], Takaharu Okada[1,2] & Jason G Cyster[1]

The mechanism of B cell–antigen encounter in lymphoid tissues is incompletely understood. It is also unclear how immune complexes are transported to follicular dendritic cells. Here, using real-time two-photon microscopy we noted rapid delivery of immune complexes through the lymph to macrophages in the lymph node subcapsular sinus. B cells captured immune complexes by a complement receptor–dependent mechanism from macrophage processes that penetrated the follicle and transported the complexes to follicular dendritic cells. Furthermore, cognate B cells captured antigen-containing immune complexes from macrophage processes and migrated to the T zone. Our findings identify macrophages lining the subcapsular sinus as an important site of B cell encounter with immune complexes and show that intrafollicular B cell migration facilitates the transport of immune complexes as well as encounters with cognate antigen.

An essential first step in antibody responses is for B cells to come in contact with the antigen. At any time, most B cells in the body are situated in lymphoid follicles in secondary lymphoid tissues. In lymph nodes, follicles are located immediately beneath the subcapsular sinus (SCS). Early studies of antigen capture in lymph nodes showed that much of the antigen is degraded in the medullary region but smaller amounts arrive in the lymphoid follicles and can be retained there on follicular dendritic cells (FDCs) for long periods[1–3]. This retention is most prominent when the antigen is able to form immune complexes[4,5], and the principal receptor systems involved in retaining antigens on FDCs are the complement receptors CR1 and CR2 (which bind active C3 and C4) and Fcγ receptor II (FcγRII)[6,7]. Separate studies have established that antigen in the form of immune complexes is typically more potent than free antigen in promoting antibody responses[8]. Thus, a model has emerged in which B cells travel to follicles to 'survey' for antigen displayed on the surfaces of FDCs.

As FDCs expressing CR1 and CR2 are situated in the central region of lymphoid follicles, the issue arises of how immune complexes that arrive in the SCS of the lymph node are delivered to FDCs. Studies have indicated that immune complexes do not travel freely into the parenchyma of lymphoid tissues[5,9–11]. In contrast to the fate of antigens captured by medullary macrophages, antigens or immune complexes captured by macrophages in SCS regions adjacent to follicles are not rapidly degraded[5,9]. Some of these SCS macrophages have been noted to extend from the SCS into the follicle and others have been found in the follicle, and the idea of an antigen-transport cell has emerged[3,5,9,12]. In time-course experiments of many hours' duration, macrophages have been noted to move from a subcapsular

location into the center of the follicle after some types of immunization[13,14]. However, such experiments have not directly demonstrated the contribution of migrating macrophages or other cell types to the transport of immune complexes and their deposition on FDCs.

Although immune complexes are displayed for prolonged periods on the surfaces of FDCs, it has remained unclear whether these cells are the main site of antigen encounter in lymphoid tissues. Additional modes of B cell–antigen encounter include direct binding of diffusing soluble antigen[15] and encounter with intact antigen displayed by classical DCs[16]. In addition to their physical proximity to FDCs, follicular B cells have close proximity to SCS macrophages[9,10]. However, the extent to which B cells capture antigen or immune complexes from SCS macrophages has not been directly assessed.

Here we have taken advantage of the ability of deep-tissue two-photon microscopy and in vivo–generated brightly fluorescent phycoerythrin-labeled immune complexes (PE-ICs) to allow tracking of the capture and transport of immune complexes in real time. We demonstrate that SCS macrophages rapidly captured PE-ICs from the afferent lymphatic flow. Many of these cells projected large processes across the floor of the SCS into the follicle, and PE-ICs were delivered along the length of these processes. B cells captured immune complexes from macrophage processes and then carried the complexes through the follicle. The capture of immune complexes by B cells and their delivery to FDCs required the expression of complement receptors by the B cells. We thus identify follicular B cells as antigen-transport cells. Finally, antigen-specific B cells were able to encounter immune complexes on SCS macrophage processes through their B cell antigen receptor (BCR) and then migrate to the T zone–B zone boundary.

[1]Howard Hughes Medical Institute and Department of Microbiology and Immunology, University of California, San Francisco, California 94143, USA. [2]Present address: Department of Synthetic Chemistry and Biological Chemistry, Graduate School of Engineering, Kyoto University, Katsura Campus, Nishikyo-ku, Kyoto, Japan. Correspondence should be addressed to J.G.C. (jason.cyster@ucsf.edu).
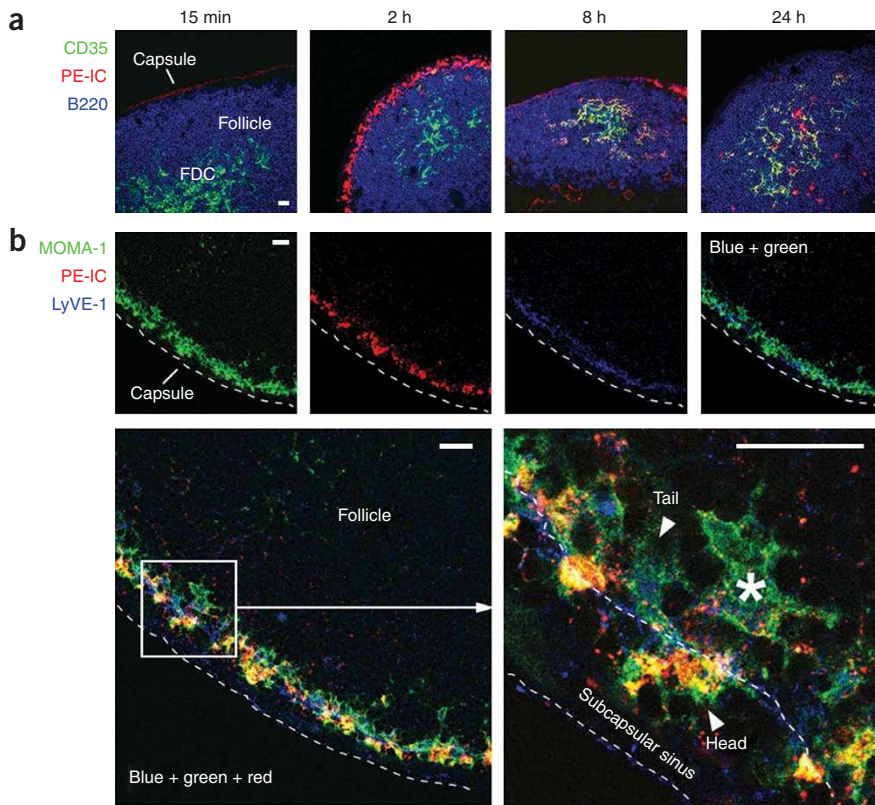
Figure 1 Deposition of PE-ICs occurs in distinct phases. Localization of immune complexes containing phycoerythrin, IgG anti-phycoerythrin and complement (PE-ICs) at 15 min, 2 h, 8 h and 24 h after phycoerythrin injection. (**a**) Confocal microscopy of draining lymph nodes stained with anti-CD35 (green) and anti-B220 (blue). Scale bar, 20 μm. Data are representative of follicles from five inguinal lymph nodes analyzed in three experiments. (**b**) Microscopy of draining lymph nodes collected 2 h after phycoerythrin injection and stained with anti-MOMA-1 (green) and anti-LyVE-1 (blue) for the identification of sinus-lining cells that had captured PE-ICs. The SCS is lined by a discontinuous layer of LyVE-1+ cells interrupted by MOMA-1+ macrophages. The boxed area at left (bottom row) is enlarged at right, which shows PE-ICs captured on the 'head' of a macrophage located in the lumen of the SCS and extending a long process ('tail') through the LyVE-1+ cell layer into the follicle. The large cell process marked with an asterisk connects to a luminal 'head' region in a deeper z-plane. Scale bars, 20 μm. Data are representative of three experiments.

RESULTS

Kinetics of the appearance of immune complexes

To develop a method that would allow the identification of the cells involved in the transport of immune complexes to FDCs, we sought to determine whether we could track the appearance and deposition of immune complexes containi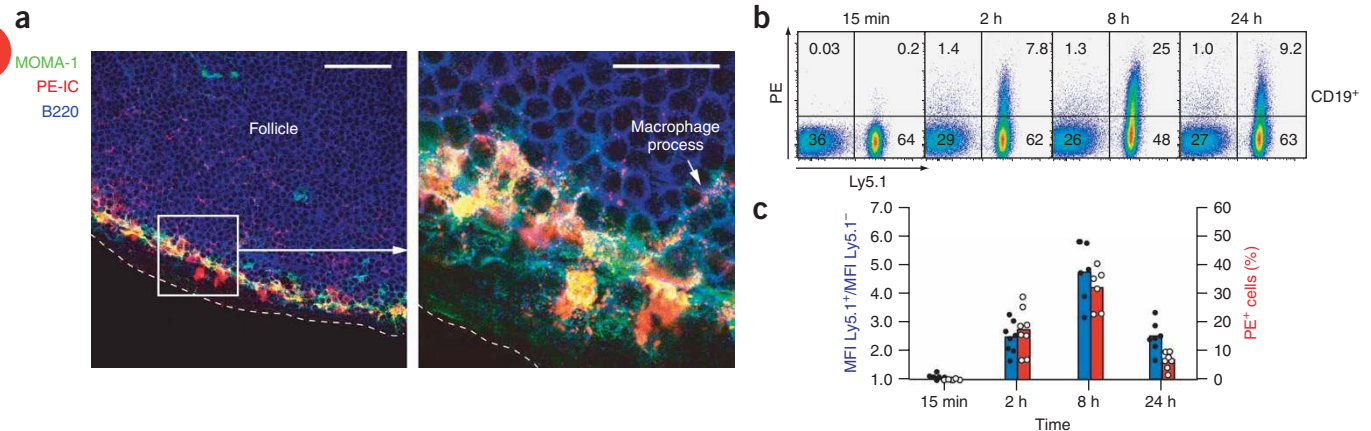ng the brightly fluorescent protein phycoerythrin. We first passively immunized mice with polyclonal antibodies specific for phycoerythrin and then gave them a subcutaneous injection of phycoerythrin to generate PE-ICs *in vivo*. This strategy resulted in robust complement-dependent deposition of PE-ICs containing phycoerythrin, antibody to phycoerythrin (anti-PE) and complement C3 (**Supplementary Fig. 1** online). Within 15 min of injection, we detected phycoerythrin signal in the subcapsular region of the draining lymph node (**Fig. 1a**). By 2 h, the phycoerythrin signal had increased and both the subcapsular macrophages (**Fig. 1**) and the medullary macrophages (data not shown) had

Figure 2 Kinetics of the capture of PE-ICs by B cells in the follicle. (**a**) Microscopy of draining lymph nodes collected 2 h after phycoerythrin injection and stained with anti-MOMA-1 (green) and anti-B220 (blue) to show PE-ICs on B cells near the SCS. Boxed area at left is enlarged at right. Arrow (right) indicates a macrophage process loaded with PE-ICs extending into the follicle. Scale bars, 20 μm. Data are representative of follicles from five inguinal lymph nodes in three experiments. (**b**) 'Pseudo-color' plots gated on CD19+ B cells, showing the phycoerythrin signal on Ly5.1+ B cells from mice given PE-ICs and control Ly5.1− B cells (added *ex vivo*). Numbers in quadrants indicate percent cells in each. Data are representative of at least five inguinal lymph nodes from two experiments. (**c**) Ratio of the geometric mean fluorescent intensity (MFI) of the phycoerythrin signal on Ly5.1+ B cells to that on Ly5.1− control B cells (filled circles; blue bars) and percent phycoerythrin-positive (PE+) cells (open circles; red bars) with the gates in **a**. To account for the *ex vivo* capture of PE-ICs, the percent phycoerythrin-positive cells was calculated by subtraction of the percent Ly5.1− control B cells that had acquired phycoerythrin from the percent Ly5.1+ B cells from phycoerythrin-injected mice that had acquired phycoerythrin. Each data point (circle) represents one inguinal lymph node; bars indicate the mean. Data are pooled from two experiments.
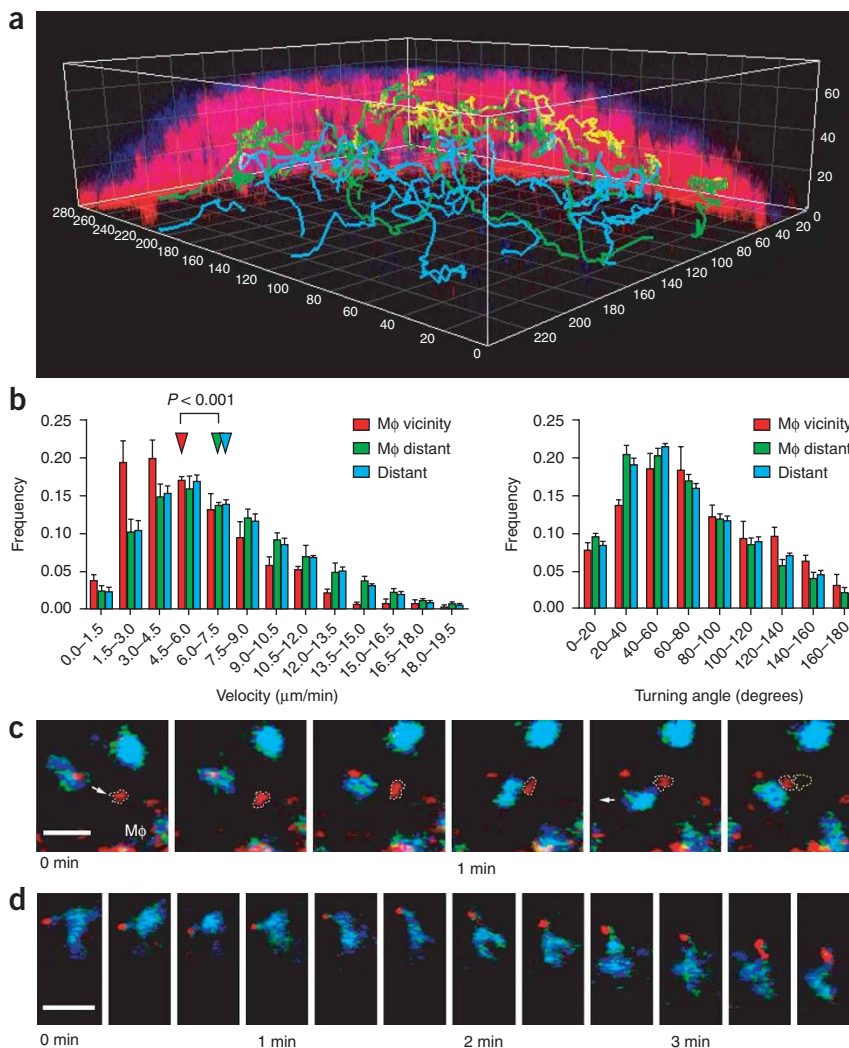
Figure 3 Dynamic capture and transport of PE-ICs by B cells. (**a**) Three-dimensional reconstruction of the follicle imaged in **Supplementary Movie 2**. The capsule is faintly visible in blue (collagen second harmonic); PE-IC$^+$ SCS macrophages are red. Green tracks represent CFP$^+$ cells that come within 10 μm of the center coordinates of the macrophages; in some areas these tracks are in such close proximity with the PE-IC that they appear yellow. Cyan tracks indicate cells that do not approach within 10 μm of PE-IC$^+$ macrophages. Grid lines are 20 μm apart. Data are representative of three experiments. (**b**) Velocities and turning angles of CFP$^+$ B cells imaged 3–4 h after phycoerythrin injection. Red, cells within 10 μm of (and possibly contacting) PE-IC$^+$ macrophages (Mφ vicinity); green, cells at least 10 μm away from PE-IC$^+$ macrophages (Mφ distant); cyan, cells that do not approach within 10 μm of PE-IC$^+$ macrophages during the imaging sequence (Distant). Triangles indicate median velocity. Range of median velocity and turning angle (three experiments): Mφ vicinity, 4.4–5.9 μm/min and 66–78°; Mφ distant, 6.2–7.8 μm/min and 55–64°; Distant, 6.2–6.8 μm/min and 58–61°. (**c**) Time-lapse images of a CFP$^+$ B cell approaching and capturing a large immobile depot of PE-IC (dashed white outlines) presumably associated with the nearby SCS macrophage (Mφ), as presented in **Supplementary Movie 3**. The first three video frames include a PE-IC in the z-stack above the B cell. Dashed yellow lines (far right) indicate the position of the PE-IC in the previous frame. Arrows indicate the direction of the cell. (**d**) Time-lapse images of a migrating CFP$^+$ B cell (cyan) carrying a large PE-IC (red) at its uropod, as presented in **Supplementary Movie 4**. Scale bars (**c,d**),10 μm; frames are 20 s apart. Data (**c,d**), are representative of three experiments.

become heavily labeled. By 8 h, phycoerythrin was readily detectable on CD35$^+$ FDCs and the signal continued to accumulate on FDCs over the next 16 h while mostly disappearing from the subcapsular region. To more closely examine the deposition and location of the early accumulating PE-ICs, we stained sections for MOMA-1, a marker of SCS macrophages, and for LyVE-1, a lymphatic marker[17] that is weakly expressed by the cells that line the SCS (**Fig. 1b**). By confocal microscopy it was evident that the subcapsular wall was composed of discontinuous rows of subcapsular macrophages interdigitated with LyVE-1$^+$ subcapsular lining cells, with parts of the macrophages projecting into the subcapsular sinus (the 'heads') and parts extending across the sinus wall and into the follicle below (the 'tails'). We found fairly uniform distribution of macrophages with these characteristics along the sinus. At 2 h after phycoerythrin injection there was considerable accumulation of PE-ICs on macrophage 'heads' and smaller amounts of PE-ICs on the intrafollicular projections of the cells (**Fig. 1b**). The PE-ICs were often distributed at the perimeter of the cell processes, most likely displayed on the cell surface (**Fig. 1b**), consistent with published findings that SCS macrophages are poorly phagocytic[5,9]. We then used intravital two-photon microscopy to examine the dynamics of the accumulation of PE-ICs on the SCS macrophages (**Supplementary Movie 1** online). Within 5 min of phycoerythrin injection, we detected a steady stream of

bright phycoerythrin fluorescence moving through the SCS in the fluid (lymph) phase. In some cases we visualized the PE-ICs as large supramolecular complexes. Very soon after this PE-ICs began to 'decorate' cell processes in the floor of the SCS that most likely corresponded to the 'heads' of SCS macrophages. Some cells accumulated PE-ICs more rapidly than others, possibly because they were better positioned in the lymph flow to capture the larger complexes as they entered from the afferent lymphatic vessel. Notably, although SCS macrophages rapidly and extensively captured PE-ICs in real time, they only rarely left the SCS and migrated deep into the follicle within the first 8 h after phycoerythrin injection (data not shown).

Follicular B cells capture PE-ICs from SCS macrophages

By close analysis of lymph node sections obtained 2 h after phycoerythrin injection, in addition to macrophage labeling, we detected many 'specks' of phycoerythrin signal throughout the region of the follicle proximal to the SCS (**Fig. 1b**). In confocal sections also stained for the B cell marker B220, it seemed that many of these puncta of phycoerythrin signal were on the surfaces of B cells (**Fig. 2a**). Moreover, in some cases, we found B cells in close juxtaposition to MOMA-1$^+$ macrophage processes 'decorated' with PE-ICs (**Fig. 2a**). Quantitative flow cytometry showed that about 15% of lymph node B cells were coated with PE-ICs by 2 h and about 40% were coated by
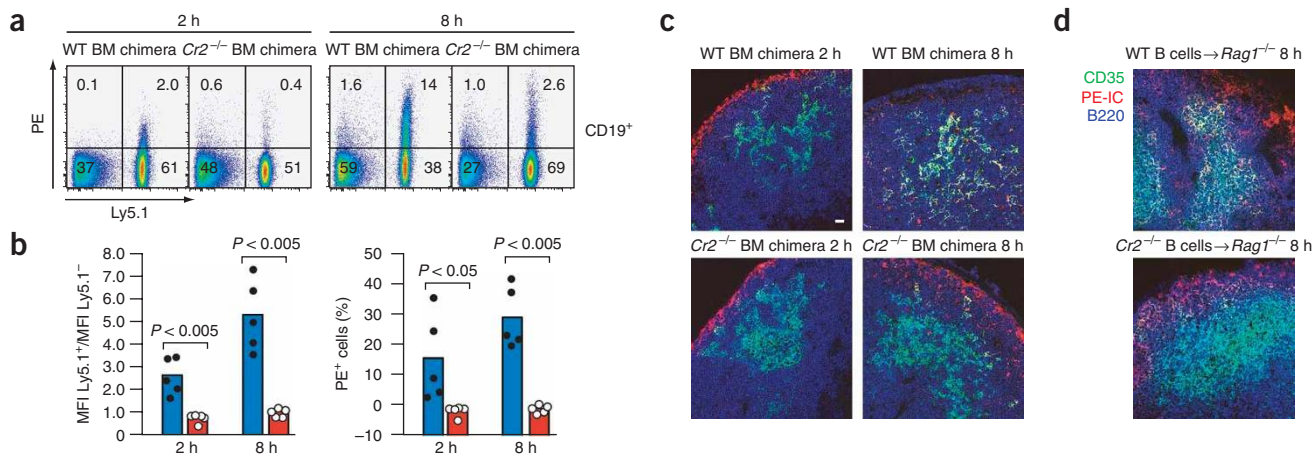
Figure 4 Expression of CR1 and CR2 by B cells is required for PE-IC capture and FDC deposition. (**a**) 'Pseudo-color' plots gated on CD19^{+} B cells, showing phycoerythrin signals on Ly5.1^{+} chimeric B cells from mice given PE-ICs and control Ly5.1^{−} B cells (added *ex vivo*). Numbers in quadrants indicate percent cells in each. WT, wild-type; BM, bone marrow. Data are representative of five mice analyzed in two experiments. (**b**) Ratio of the mean fluorescent intensity of the phycoerythrin signal on Ly5.1[+] chimeric B cells to that on control Ly5.1^{−} B cells, and the percent phycoerythrin-positive cells with the gates in **a**. Filled circles and blue bars, wild-type bone marrow chimeras; open circles and red bars, *Cr2*^{−/−} bone marrow chimeras. Each data point (circle) represents one inguinal lymph node; bars indicate the mean. Data are pooled from two independent experiments. (**c**,**d**) Microscopy of draining lymph nodes from bone marrow–chimeric mice (**c**) or mice deficient in recombination-activating gene 1 (*Rag1*^{−/−}) that had received transferred B cells (**d**); lymph nodes are stained with anti-CD35 (green) and B220 (blue). Scale bar, 20 μm. Data are representative of follicles from four inguinal lymph nodes of each type, analyzed in two experiments.

8 h; this 'decayed' to about 10% by 24 h (**Fig. 2b,c**). In these experiments, we processed draining lymph nodes together with untreated Ly5.2 congenic control lymph nodes to exclude the possibility of *ex vivo* capture of the PE-ICs (**Fig. 2b,c**).

To examine the migration dynamics of B cells that captured PE-ICs, we obtained draining lymph nodes from mice in which 0.5–1% of the follicular B cells expressed cyan fluorescent protein (CFP) under the control of a β-actin promoter[18] and analyzed the lymph nodes by two-photon microscopy. In time-lapse image sequences collected beginning at 3 h after phycoerythrin injection (**Supplementary Movie 2** online), CFP^{+} B cells were motile and often migrated to the subcapsular region and contacted several PE-IC–loaded macrophages before returning to the follicle (**Supplementary Movie 2** and **Fig. 3a**). By tracking analysis, the cells had lower migration velocities and greater turning angles when in the vicinity of the PE-IC[+] macrophages, consistent with the cells' undergoing close interactions (**Fig. 3a,b**). In the subcapsular region, many motile 'specks' of phycoerythrin were visible; some of these were very large. By focusing in this region, we found that after coming into contact with SCS macrophages, some of the labeled B cells had acquired phycoerythrin on their surface (**Supplementary Movie 3** online). Rare labeled B cells encountered a large immobile depot of PE-ICs (most likely macrophage associated) and slowed down before migrating away with the PE-ICs attached, at least for a short time (**Supplementary Movie 3** and **Fig. 3c**). Furthermore, by 4 h after injection of phycoerythrin, follicular B cells had acquired a dendritic morphology reminiscent of that described for germinal center B cells[19] and migrated with PE-ICs attached on their surface, typically most concentrated at the trailing edge (uropod) of the migrating cell (**Supplementary Movie 4** online and **Fig. 3d**). Thus, migrating follicular B cells can serve as antigen-transport cells by transporting immune complexes from the SCS into the follicle.

B cell capture of PE-ICs depends on complement receptor
As the PE-ICs contained C3 (**Supplementary Fig. 1**) and all follicular B cells seemed able to capture PE-ICs, it was likely that they used
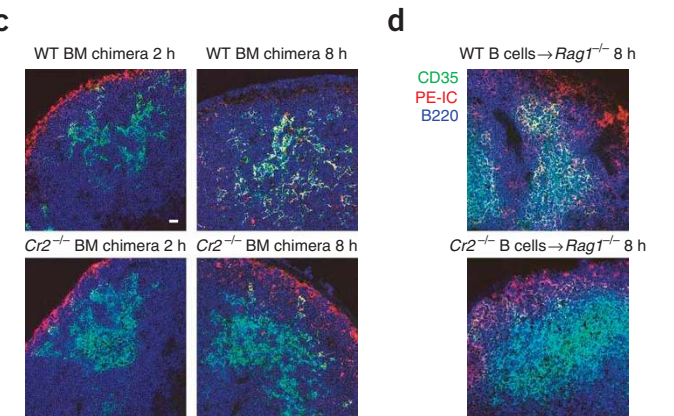
either complement or Fc receptors for this process. To assess the requirement of B cells for CR1 and CR2, we reconstituted lethally irradiated wild-type C57BL/6 mice with *Cr2*^{−/−} (ref. 20) bone marrow such that hematopoietic cells lacked these complement receptors, whereas they continued to be expressed by radiation-resistant FDCs. Flow cytometry showed considerable impairment in the ability of B cells deficient in CR1 and CR2 to capture PE-ICs at 2 h and 8 h (**Fig. 4a,b**). Notably, their inability to capture PE-ICs resulted in impaired transport of PE-ICs into the follicle from the subcapsular space at 2 h and substantial delay in FDC deposition at 8 h (**Fig. 4c**). To confirm that the impaired follicular access of PE-ICs was specifically dependent on expression of CR1 and CR2 by B cells, we isolated B cells from *Cr2*^{−/−} or wild-type chimeric mice and adoptively transferred them into C57BL/6 hosts deficient in recombination-activating gene 1 that lack B cells and T cells. Confocal image analysis 8 h after injection of phycoerythrin into recipients of *Cr2*^{−/−} B cells showed considerable delay in FDC deposition, as noted for the *Cr2*^{−/−} radiation chimeras (**Fig. 4d**). Next we labeled *Cr2*^{−/−} and wild-type follicular B cells with the fluorescent dye CFSE (carboxyfluorescein diacetate succinimidyl ester) and analyzed the cells by two-photon microscopy. Time-lapse images obtained 3 h after the injection of phycoerythrin confirmed that B cells deficient in CR1 and CR2 did not capture PE-ICs, in contrast to wild-type B cells (**Supplementary Movie 5** online). The B cells deficient in CR1 and CR2 projected dendritic extensions similar to those of wild-type B cells, suggesting that the morphological change was independent of B cell–intrinsic complement receptor–derived signals (**Supplementary Movie 5**). These findings demonstrate that the capture and transport of noncognate immune complexes by B cells is complement receptor-dependent.

B cells capture cognate antigen from SCS macrophages
The efficient capture of PE-ICs by B cells in the subcapsular region suggested that this may also be a potential site for cognate B cells to encounter opsonized antigens. To test that possibility, we covalently
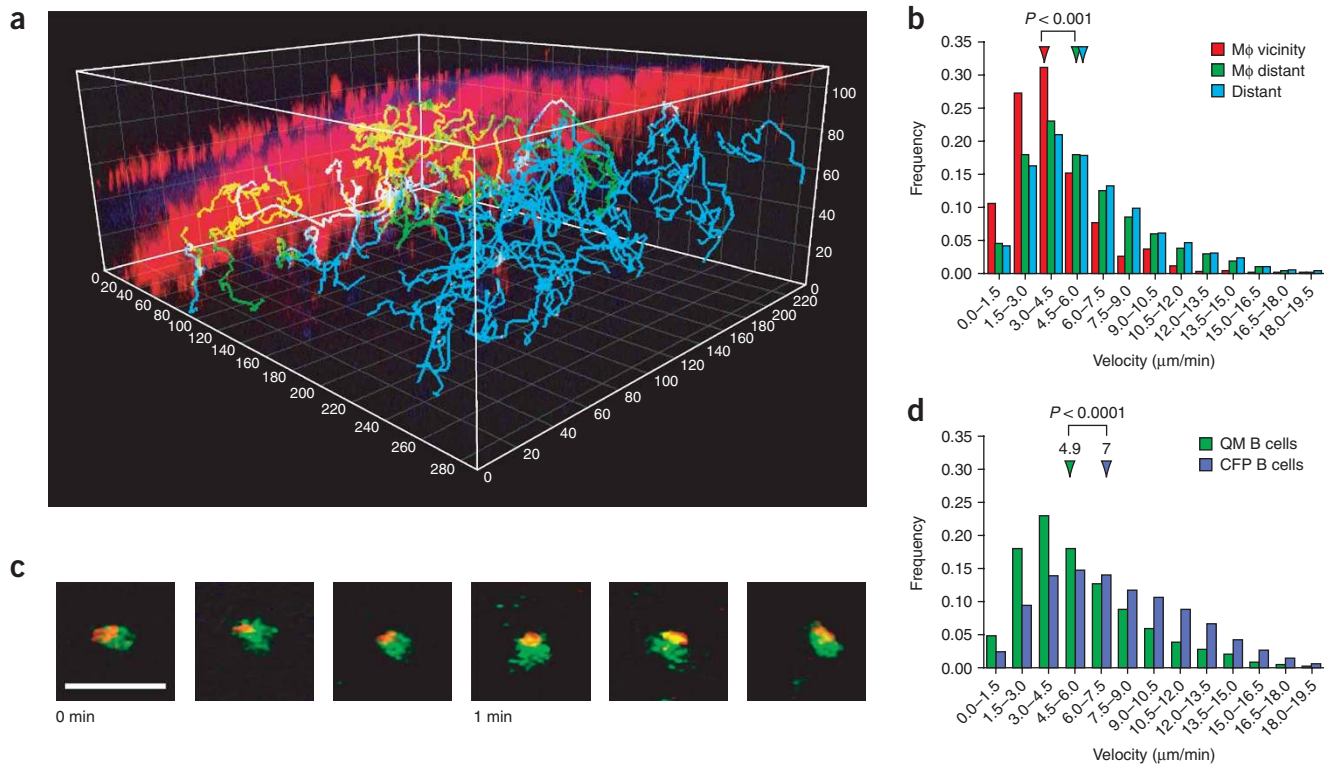
Figure 5 Dynamic capture and transport of immune complexes by cognate B cells. (**a**) Three-dimensional reconstruction of the follicle imaged in **Supplementary Movie 6**. Tracks belong to QM B cells defined in relation to PE-IC[+] macrophages as in **Figure 3a**. Grid lines are 20 μm apart. The separate layer of phycoerythrin signal on the left belongs to the SCS of an adjacent follicle. (**b**) Velocity of cognate QM B cells in the follicle 2nd subcapsular region. Key is as described in **Figure 3b**. Triangles indicate median velocity (colors match key): red, 3.6 μm/min; green, 4.8 μm/min; cyan, 5.1 μm/min. Similar results were obtained in two experiments. (**c**) Time-lapse images showing a CFSE-labeled QM B cell (green) carrying large NP-PE–ICs (orange) capped at the uropod as presented in **Supplementary Movie 6**. Scale bar, 20 μm. Data are representative of two experiments. (**d**) Velocities of cognate QM B cells and noncognate CFP^{+} B cells imaged 3 h after injection of NP-PE. Triangles indicate median velocity (in μm/min). Similar results were obtained in two experiments.

conjugated phycoerythrin to the hapten nitrophenyl (NP-PE) and used that to generate NP-PE–labeled immune complexes (NP-PE–ICs) *in vivo*. We then fluorescently labeled nitrophenyl-specific B cells from a 'quasi-monoclonal' (QM) mouse[21] with CFSE, transferred the cells together with wild-type CFP^{+} B cells and analyzed them by two-photon microscopy. Time-lapse images obtained 3 h after injection of NP-PE showed QM B cells migrating to and slowing down on contact with SCS macrophages, as noted for noncognate CFP^{+} B cells (**Supplementary Movie 6** online and **Fig. 5a,b**). However, these images were notable for the more efficient capture of NP-PE–ICs from SCS macrophages by QM B cells relative to the capture by polyclonal CFP^{+} B cells. Indeed, most QM B cells migrated with large NP-PE–ICs capped at the uropod by 3 h after injection of NP-PE (**Supplementary Movie 6** and **Fig. 5c**). These immune complexes had a higher image intensity than that noted for immune complexes carried by noncognate B cells. Cognate B cells, in contrast to polyclonal B cells, migrated with less dendritic morphology (**Supplementary Movie 6** and **Figs. 3d** and **5c**). Furthermore, the tracked QM B cells had lower motility, similar to that described before, at 1–3 h after BCR ligation of transgenic B cells (**Fig. 5d**)[19]. Flow cytometry confirmed the rapid and efficient capture of immune complex–coated antigen by cognate QM B cells (**Fig. 6a,b**). In comparison to capture of PE-ICs by both wild-type and QM B cells, which peaked at 8 h (**Fig. 2b** and **Fig. 6a**), capture of NP-PE–ICs by QM B cells was already maximal by 2 h (**Fig. 6a**). Moreover, the geometric mean fluorescence

intensity of the phycoerythrin signal at 2 h was much greater for NP-PE–ICs (about 1,400) than for PE-ICs (about 160), indicating that QM B cells had captured more cognate immune complexes in a shorter period of time, as also evident in the real-time two-photon microscopy (**Supplementary Movies 3** and **6**). This effect was antigen specific, as there was no difference in the capture of noncognate PE-ICs by QM B cells and wild-type B cells (**Fig. 6a**). Capture of cognate immune complexes was mediated by the BCR, as about 40–50% of QM B cells had upregulated expression of the costimulatory molecule B7.2 (CD86) as early as 8 h, compared with 10–20% at 2 h after injection of NP-PE (**Fig. 6b**). In contrast, capture of noncognate PE-ICs by QM B cells over this time period did not lead to upregulation of B7.2 above the baseline frequency of 10–20%. In control experiments in which we added CFSE-labeled QM B cells to lymph node samples during tissue preparation for flow cytometry, we also noted *ex vivo* BCR-mediated capture of NP-PE–ICs, but this did not reach the same extent as that achieved *in vivo* (**Fig. 6c**) and did not result in induction of B7.2 (**Fig. 6d**). Finally, QM B cells were excluded from the follicle and relocalized to the T zone by 24 h after administration of NP-PE–ICs, consistent with crosslinking of the BCR by cognate antigen (**Fig. 6e**). In contrast, QM B cells were evenly distributed throughout the follicle at 24 h after the administration of noncognate PE-ICs (**Fig. 6e**). Thus, SCS macrophages can present native antigen to naive follicular B cells in the form of immune complexes and activate the B cells.
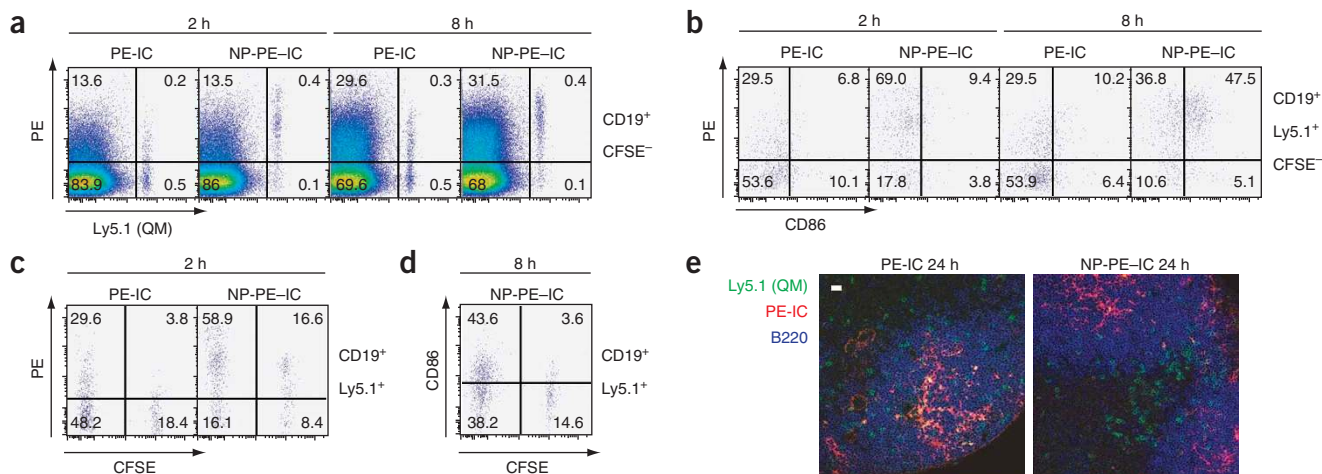
Figure 6 Cognate B cells efficiently capture opsonized antigen from SCS macrophages and become activated. (**a**) 'Pseudo-color' plots of phycoerythrin signal intensity on QM (Ly5.1^{+}) and wild-type (Ly5.1^{−}) inguinal lymph node B cells gated on CD19^{+} cells, excluding CFSE-labeled QM cells used as *ex vivo* mixing controls; times above plots indicate isolation time after injection of phycoerythrin or NP-PE. (**b**) 'Pseudo-color' plots of phycoerythrin signal intensity and CD86 expression on QM B cells pregated on Ly5.1 as described in **a**. (**c,d**) 'Pseudo-color' plots of CD19^{+}Ly5.1^{+} CFSE^{−} QM B cells from mice containing immune complexes as well as control CFSE^{+} QM B cells (added *ex vivo*), showing phycoerythrin signal intensity (**c**) and CD86 expression (**d**). Numbers in quadrants (**a–d**) indicate percent cells in each. Data are representative of at least five mice in each group in two experiments. (**e**) Microscopy of draining lymph nodes stained with Ly5.1 (green) to identify QM cells and either anti-B220 (blue) or anti-CD4 (blue) to delineate the T zone–B zone boundaries in mice given phycoerythrin or NP-PE 24 h earlier. Scale bar, 20 μm. Data are representative of follicles from four inguinal lymph nodes of each type in two experiments.

DISCUSSION

We have demonstrated here that immune complexes captured by SCS macrophages are picked up by migrating follicular B cells by means of CR1 and/or CR2 and are delivered to FDCs, establishing B cells as an important type of antigen-transport cell in lymph nodes. Our experiments have also shown that B cells can capture cognate antigen by means of their BCR directly from SCS macrophages. These results add to earlier findings to suggest that SCS-associated macrophages are important in the presentation of immune complexes and possibly other forms of antigen for encounter and capture by follicular B cells.

The mechanism of antigen capture in lymph nodes and delivery to FDCs has been under investigation for more than 40 years[22,23]. A common theme in early studies was the observation that large amounts of antigen and immune complexes arriving in lymph nodes are taken up and degraded by medullary macrophages, whereas smaller amounts are picked up by cells associated with the SCS[1,5,9]. Notably, the SCS cells have been found to have limited phagocytic activity, in contrast to the medullary cells, and to retain antigen on their surface[5,9]. Our findings are in agreement with the conclusion that the SCS macrophages are poorly phagocytic and instead retain immune complexes on their surface for hours. Alternatively, the cells may internalize the complexes and rapidly recycle them back to the surface, possibly at the opposite pole of the cell. The mechanisms promoting the retention of immune complexes by these cells are not yet apparent but may involve FcγRII, a receptor that can allow the capture and recycling of immune complexes[24], or the C3b receptor Mac-1 (CD11b-CD18). Several electron microscopy studies have noted that the SCS macrophages often penetrate the SCS lining cells[5,9,12], though it is unclear whether the cells were in transit or were stably positioned. By combining confocal and dynamic imaging approaches here, we have been able to establish that many of these

cells do project through the cellular lining of the SCS and that they are stably situated in this location.

An important principle that has emerged during studies tracking the distribution of labeled antigens in lymphoid tissues has been the existence of a sieving mechanism that limits the access of antigen and immune complexes to the tissue parenchyma[5,9,11]. A study examining the distribution of labeled molecules varying in molecular weight and hydrodynamic radius has concluded that molecules with a hydrodynamic radius larger than 5.5 nm (or approximately 70 kilodaltons) are excluded from freely accessing the parenchyma of the tissue and that smaller antigens can gain access to fluid-filled conduits but not the tissue parenchyma[11]. Another study has provided evidence that some types of soluble antigen may gain direct (and selective) access to the follicle for immediate capture via the BCR of antigen-specific cells[15]. This last study pointed out that soluble antigen may have been missed in earlier work because it was washed away from the tissue during preparation and staining. The immune complexes we examined here did not gain free access to the follicle, as they failed to efficiently 'decorate' FDCs when the B cells lacked CR1 and CR2. Moreover, time-course imaging analysis indicated that the rate of immune complex spread through the follicle was consistent with the rate of B cell migration from the SCS region and dispersal through the follicle. Thus, our findings are consistent with earlier work indicating that immune complexes and molecules larger than antibodies do not readily gain free access to follicles and support the conclusion that they will typically be transported by cells.

Early studies of the capture and deposition of systemic immune complexes in the spleen provided evidence that they can be detected on the surface of lymphocytes, some of which seem to be migrating from the marginal zone into the follicle[25]. Several studies have shown that treatments such as lipopolysaccharide or exposure to pertussis

toxin, which cause displacement of marginal zone B cells, reduce the efficiency of immune complex delivery to FDCs[26–28]. However, such treatments also affect other cell types, and such work has not yet definitively established the idea that marginal zone B cells are the main immune complex–transport cells in the spleen. The idea that B cells may be able to transport immune complexes was also indicated by an early study showing that intravenous transfer of B cells coated with aggregated immunoglobulin G (IgG) leads to more efficient deposition of the IgG in splenic follicles than occurs after direct injection of aggregated IgG[29]. Beyond those studies, the function of B cells as antigen-transport cells in tissues other than the spleen has rarely been explored. The idea of a 'conveyer belt' mechanism for antigen transport from the SCS to FDCs has been discussed[9,10], but at that time the high motility of B cells was not appreciated and thus their potential involvement in antigen transport was difficult to envisage. One electron microscopy study did detect immune complexes on the surfaces of lymph node B cells shortly after antigen injection and before their appearance on FDCs[30]. Our studies have now established that follicular B cells capture immune complexes *in vivo* through surface complement receptors and that such capture is important in the transport of antigen to FDCs in lymph nodes. Evidence that B cells that have bound noncognate immune complexes can 'give up' the immune complexes to FDCs has been obtained through *in vitro* studies[30]. In addition, when mice are injected with antibody specific for CR1 and CR2, it is initially concentrated on B cells in the spleen, but after several hours the antibody becomes concentrated on FDCs and there is less on B cells[31]. FDCs have much more expression of CR1 and CR2 than follicular B cells do[6]; this probably ensures that they compete successfully with migrating B cells for the capture and retention of noncognate immune complexes. As well as migrating through the FDC network of primary follicles and the mantle zones of secondary follicles, naive B cells have been found to migrate in and out of the FDC-rich light zone of germinal centers[19,32]. Given those findings, together with our studies here, it can be suggested that naive B cells are involved in the ongoing delivery of immune complexes to light-zone FDCs during the germinal center response.

Although our work has demonstrated that follicular B cells can transport immune complexes, we have not ruled out the possibility that other cell types function as antigen-transport cells in some circumstances. SCS macrophages have been reported to migrate into follicles after some immunizations[13,14]. Similarly, the related marginal-zone macrophages of the spleen migrate into follicles after exposure to lipopolysaccharide[27]. That process is slower than the transport mechanism we have described here, taking many hours, but it may be involved in the transport of different types of antigens.

Priming or passive antibody transfer can considerably augment antibody responses[8]. Our findings are consistent with the proposal that one reason for this is that the antibody facilitates the formation of 'complement-decorated' immune complexes, thereby promoting the capture of antigen and its delivery into follicles, as well as encounter by the few follicular B cells that are antigen specific. Although our model system used IgG antibodies to form immune complexes, we envisage that the complement-dependent capture and transport of immune complexes we have reported here also applies to immune complexes formed by natural IgM antibodies in antigen-naive animals[33,34]. It seems likely that the same mechanisms will operate for antigens that become coated with complement through the antibody-independent alternative or lectin pathways. Additional receptor systems that recognize innate features of pathogens may also participate in antigen capture and display by SCS macrophages.

The follicle has long been considered a chief site of B cell–antigen encounter, with FDCs being important in displaying antigen in the form of immune complexes to B cells. However, the relative importance of FDCs in fostering the encounter of B cells with antigen in the early phases of the B cell response remains to be determined. Additional modes of B cell–antigen encounter in lymphoid tissues have been demonstrated that involve encounter with soluble antigen freely entering the follicle and encounter with antigen on T zone DCs[15,16]. Our studies have demonstrated that SCS macrophages are another important site of antigen display and encounter by cognate B cells. Indeed, in our experiments in which we provided antigen as a single bolus injection (typical of vaccination), most of the antigen-specific B cells in the draining lymph node acquired antigen before the appearance of the antigen on FDCs. We anticipate that during infection, antigenic material would continue arriving in the draining lymph node for many hours or days and that there would be ongoing display of newly generated immune complexes by SCS macrophages. Therefore, we suggest that these specialized macrophages may be a prominent site for naive B cells to encounter a variety of antigen types. The related population of macrophages in the splenic marginal zone also sends projections into the underlying follicles and may have a similar function[35]. Our studies also suggest an additional mode of encounter with cognate antigen in which antigen-specific B cells capture immune complexes from noncognate antigen–transporting B cells as the cells migrate in among each other in the tightly packed lymphoid follicle. Finally, the high immune complex–binding capacity of FDCs probably helps to relieve noncognate B cells of all their immune complex 'cargo' before they exit the lymph node, helping to ensure that the immune response is mounted locally rather than systemically. Efficient capture of immune complexes by FDCs may also be important in limiting the dispersal of bacteria, viruses and prions, and defects in this process might be a basis for the B cell–mediated spread of disease-causing agents.

METHODS

Mice. Female wild-type and Ly5.2 (CD45.1) congenic C57BL/6 mice 6–12 weeks old were from the National Cancer Institute or Jackson Laboratories. C57BL/6 mice expressing CFP under control of the β-actin promoter (004218; Tg(ACTB-ECFP))[18] and mice deficient in recombination-activating gene 1 (002216: $Rag1^{tm1Mom}$)[36] were from Jackson Laboratories. Mice deficient in CR1 and CR2 and QM mice expressing a 'knocked-in' BCR specific for nitrophenyl ($V_H17.7.25 \times J_H$-deficient × κ-deficient) have been described[20,21]. Mice were housed in germ-free environment in the Laboratory Animal Research Center at the University of California at San Francisco and all experiments conformed to ethical principles and guidelines approved by the Institutional Animal Care and Use Committee of the University of California at San Francisco.

Bone marrow chimeras and B cell reconstitutions. Wild-type mice were lethally irradiated with 1,100 rads in split doses and were reconstituted with 1×10^6 bone marrow cells from $Cr2^{-/-}$ or wild-type donors. Chimeric mice were analyzed 8–10 weeks later. For the production of mice deficient in CR1 and CR2 only in the B cell compartment, B cells were isolated from 12-week-old chimeric mice and 100×10^6 of the cells were adoptively transferred into C57BL/6 mice deficient in recombination-activating gene 1. Mice were then analyzed 3 weeks later.

B cell isolation, CFSE labeling and adoptive transfer. For imaging, B cells were isolated from spleen and peripheral and mesenteric lymph nodes as described[19] with an AutoMACS cell separator (Miltenyi Biotech) and biotinylated monoclonal anti-CD11c (HL3), monoclonal anti-CD43 (S7; both from BD Biosciences) and MACS streptavidin microbeads (Miltenyi Biotech). B cells were enriched to over 95% purity, as confirmed by flow cytometry. For tracking of B cells from chimeras deficient in CR1 and CR2, wild-type chimeras and QM

mice, CFSE (Invitrogen Molecular Probes) was used at a concentration of 2.5 μM as described[37]. Cells (1×10^6 to 2×10^6) were adoptively transferred the day before so that transferred B cells constituted about 0.5–1% of the B cell compartment of the recipient mouse. For analysis of the acquisition of immune complex–coated antigen, 1×10^7 QM B cells were adoptively transferred into Ly5.2 congenic recipients. Some mice also received QM B cells labeled with CFSE at a concentration of 0.25 μM as controls for the *ex vivo* capture of NP-PE–ICs by the cognate BCR.

In vivo generation of immune complexes. Mice were given 2 mg polyclonal rabbit IgG anti-phycoerythrin (200-4199; Rocklands) intraperitoneally 12–16 h before subcutaneous injection of either 10 μg phycoerythrin (P-801; Invitrogen Molecular Probes) or NP-PE in the flank and tail base to drain to both medial and lateral lobes of the inguinal lymph node. For subcutaneous injection, mice were anaesthetized intraperitoneally with 100 mg per kg body weight of an anesthetic solution containing ketamine (5 mg/ml) and xylazine (1 mg/ml; both from Sigma). Similar deposition of PE-ICs was achieved with hyperimmune mouse serum to phycoerythrin (data not shown).

Complement depletion. Mice were depleted of complement by repeated intraperitoneal injection of 7.5 U cobra venom factor (Quidel) at 36, 24 and 12 h before the administration of rabbit IgG anti-phycoerythrin. Depletion was confirmed by failure to deposit trinitrophenyl-Ficoll (BioSearch Technologies) in the splenic marginal zone 30 min after intravenous injection of 50 μg trinitrophenyl-Ficoll in treated mice relative to that in control mice (data not shown).

Conjugation of nitrophenyl to phycoerythrin. Phycoerythrin (1 mg) was dialyzed overnight at 4 °C against NaHCO₃, pH 8.4, and was allowed to react for 2 h at 37 °C with 5 mg NP-OSu (4-hydroxy-3-nitrophenylacetic acid active ester; BioSearch Technologies) dissolved in 50 μl N,N-dimethylformamide with frequent vortexing. The precipitate was discarded and the reaction mixture was dialyzed for 4 h against NaHCO₃ and then was dialyzed for 1–2 d at 4 °C against PBS for the removal of 'unreacted' NP-OSu.

Flow cytometry. Draining inguinal lymph nodes were carefully collected with the removal of excess fat and connective tissue and were 'teased apart' with microforceps before being passed through a 70-μm nylon sieve (BD Biosciences) along with lymph nodes from Ly5.2 congenic mice that did not receive phycoerythrin to control for the *ex vivo* capture of PE-ICs. For NP-PE–ICs, draining lymph nodes were processed together with lymph nodes from mice containing CFSE-labeled QM cells that did not receive NP-PE. Single-cell suspensions were stained as described[19] with Pacific blue–conjugated monoclonal anti-CD19 (6D5) plus Alexa Fluor 700–conjugated anti-CD45.2 (104) or anti-CD45.1 (A20; all from BioLegend). In experiments with *Cr2⁻/⁻* bone marrow chimera, suspensions were also stained with monoclonal antibody to CD21 and CD35 (7G6; BD Biosciences). In experiments with QM B cells, suspensions were also stained with biotinylated monoclonal anti-CD86 (GL1; BD Biosciences) and were visualized with streptavidin–Alexa Fluor 647 (Invitrogen Molecular Probes). Data were acquired on a LSRII flow cytometer (BD Biosciences) and were analyzed with FlowJo software (Treestar).

Confocal microscopy. Tissue sections 10–30 μm in thickness were stained with rat monoclonal anti–mouse C3 (CL7503AP; Cedarlane), anti-CR1 (8C12) or MOMA-1 hybridoma supernatant and were detected with fluorescein isothiocyanate–conjugated anti–rat IgG (heavy plus light) F(ab′)₂ (Jackson Immunosearch). Rabbit IgG was detected with fluorescein isothiocyanate–conjugated anti–rabbit IgG (heavy plus light) F(ab′)₂ (Jackson Immunosearch). Sections were then blocked with 5% normal rat serum before being stained with biotinylated monoclonal anti-LyVE-1 (223322; R&D Systems) or with monoclonal anti-B220 (RA3-6B2; BD Biosciences) and streptavidin–Alexa Fluor 647. For analysis of the positioning of QM B cells, sections were stained with fluorescein isothiocyanate–labeled monoclonal anti-CD45.2 (104) followed by either monoclonal anti-B220 as described above or Alexa Fluor 647–conjugated monoclonal anti-CD4 (RM4-5; all from BD Biosciences). Images were acquired on a TCS SL confocal microscope (Leica Microsystems) with 488-, 543- or 633-nm laser lines for the excitation of fluorescein isothiocyanate, phycoerythrin or Alexa Fluor 647, respectively. Emission slits were 'tuned' to 498–540 nm

for fluorescein isothiocyanate, to 560–600 nm for phycoerythrin and to 643–710 nm for Alexa Fluor 647. Confocal images were processed with Adobe PhotoShop CS2.

Intravital microscopy and two-photon microscopy. For anesthesia, mice were induced intraperitoneally with 20 mg per kg body weight of anesthetic solution (ketamine (5 mg/ml) and xylazine (1 mg/ml)); maintenance doses of intramuscular injection of 20 mg per kg body weight were given every 20–30 min as needed to ensure deep anesthesia, as indicated by regular, shallow respiration and suppression of withdrawal reflexes. Anesthetized mice were given supplemental oxygen through a nose cone and were prepared for intravital microscopy as described[19]. The day before intravital microscopy, mice were given subcutaneous injection in the left flank of 20 μg of Alexa Fluor 488–conjugated anti-CD157 (BP-3) for labeling of the follicular stroma *in vivo*. Explanted lymph nodes were prepared for two-photon microscopy as described[38]. Images were acquired with a custom-built two-photon microscope. A MaiTai TiSapphire laser (Spectra-Physics) was 'tuned' to provide an excitation wavelength of 910 nm. Each *xy* plane spanned 480 × 400 pixels at a resolution of 0.6 μm per pixel, and 40–50 *xy* planes with *z* spacings of 2 μm were formed by averaging of ten video frames every 20–30 s. Emission wavelengths of 455–485 nm (CFP and second harmonic emission of collagen fibers), 500–540 nm (CFSE and Alexa Fluor 488) and 567–640 nm (PE-ICs) were collected with photomultiplier tubes (Hanamatsu). Images were acquired with Video Savant (IO Industries) and maximum-intensity time-lapse images were generated with MetaMorph (Molecular Devices). Videos were processed with a low-pass noise filter. Cell tracks and three-dimensional rotation images were made with Imaris 5.01 × 64 (Bitplane), and automated tracks were verified and corrected manually. For the tracking of B cells relative to the SCS floor, the coordinates of macrophages with acquired phycoerythrin were defined in each video frame with Imaris software as red spots with a minimum diameter of 10 μm. Cells were considered in the vicinity of macrophages if they approached within 10 μm of the designated macrophage coordinates. Tracks of cells in the vicinity of macrophages during the imaging were broken into 'macrophage-adjacent' or 'macrophage-distant' portions and were then analyzed separately, as were tracks of cells that were never in the vicinity of any macrophages. The velocities and turning angles of cells between each imaging frame were calculated with MatLab (MathWorks). Measurements were obtained for at least 70 cells in all cases. Adobe After Effects 7.0 was used for annotation and final movie compilation. Video files were converted to 'mpeg' format with AVI-MPEG Converter for Windows 1.5 (FlyDragon Software).

Statistical analysis. GraphPad Prism (GraphPad Software) was used for all statistical analyses. For comparison of multiple nonparametric data sets (CFP B cells contacting macrophages while in the vicinity and while distant, and CFP B cells not contacting macrophages), the Kruskal-Wallis test followed by Dunn's post-test comparison between multiple groups was used (**Fig. 3b**). The same analysis was used for CFSE-labeled QM B cells for analysis of their relationship to SCS macrophages (**Fig. 5b**). For comparison of two nonparametric data sets (CFSE-labeled QM B cells and CFP B cells) the Mann-Whitney U-test was used (**Fig. 5b,d**). We hypothesized that deficiency in CR1 and CR2 would impair the ability of B cells to capture PE-ICs and therefore compared the means between the two groups with the one-tailed *t*-test (**Fig. 4b**).

Note: Supplementary information is available on the Nature Immunology website.

1. Nossal, G.J., Abbot, A., Mitchell, J. & Lummus, Z. Antigens in immunity. XV. Ultrastructural features of antigen capture in primary and secondary lymphoid follicles. *J. Exp. Med.* **127**, 277–290 (1968).
2. Tew, J.G., Phipps, R.P. & Mandel, T.E. The maintenance and regulation of the humoral immune response: persisting antigen and the role of follicular antigen-binding dendritic cells as accessory cells. *Immunol. Rev.* **53**, 175–201 (1980).
3. Szakal, A.K., Kosco, M.H. & Tew, J.G. Microanatomy of lymphoid tissue during humoral immune responses: structure function relationships. *Annu. Rev. Immunol.* **7**, 91–109 (1989).
4. Nossal, G.J., Ada, G.L., Austin, C.M. & Pye, J. Antigens in immunity. 8. Localization of 125-I-labelled antigens in the secondary response. *Immunology* **9**, 349–357 (1965).
5. Fossum, S. The architecture of rat lymph nodes. IV. Distribution of ferritin and colloidal carbon in the draining lymph nodes after foot-pad injection. *Scand. J. Immunol.* **12**, 433–441 (1980).
6. Carroll, M.C. The role of complement and complement receptors in induction and regulation of immunity. *Annu. Rev. Immunol.* **16**, 545–568 (1998).
7. Qin, D. *et al.* Fcγ receptor IIB on follicular dendritic cells regulates the B cell recall response. *J. Immunol.* **164**, 6268–6275 (2000).
8. Heyman, B. Regulation of antibody responses via antibodies, complement, and Fc receptors. *Annu. Rev. Immunol.* **18**, 709–737 (2000).
9. Szakal, A.K., Holmes, K.L. & Tew, J.G. Transport of immune complexes from the subcapsular sinus to lymph node follicles on the surface of nonphagocytic cells, including cells with dendritic morphology. *J. Immunol.* **131**, 1714–1727 (1983).
10. Tew, J.G., Mandel, T.E., Phipps, R.P. & Szakal, A.K. Tissue localization and retention of antigen in relation to the immune response. *Am. J. Anat.* **170**, 407–420 (1984).
11. Gretz, J.E., Norbury, C.C., Anderson, A.O., Proudfoot, A.E. & Shaw, S. Lymph-borne chemokines and other low molecular weight molecules reach high endothelial venules via specialized conduits while a functional barrier limits access to the lymphocyte microenvironments in lymph node cortex. *J. Exp. Med.* **192**, 1425–1440 (2000).
12. Farr, A.G., Cho, Y. & De Bruyn, P.P. The structure of the sinus wall of the lymph node relative to its endocytic properties and transmural cell passage. *Am. J. Anat.* **157**, 265–284 (1980).
13. Martinez-Pomares, L. *et al.* Fc chimeric protein containing the cysteine-rich domain of the murine mannose receptor binds to macrophages from splenic marginal zone and lymph node subcapsular sinus and to germinal centers. *J. Exp. Med.* **184**, 1927–1937 (1996).
14. Mueller, C.G. *et al.* Mannose receptor ligand-positive cells express the metalloprotease decysin in the B cell follicle. *J. Immunol.* **167**, 5052–5060 (2001).
15. Pape, K.A., Catron, D.M., Itano, A.A. & Jenkins, M.K. The humoral immune response is initiated in lymph nodes by B cells that acquire soluble antigen directly in the follicles. *Immunity* **26**, 491–502 (2007).
16. Qi, H., Egen, J.G., Huang, A.Y. & Germain, R.N. Extrafollicular activation of lymph node B cells by antigen-bearing dendritic cells. *Science* **312**, 1672–1676 (2006).
17. Banerji, S. *et al.* LYVE-1, a new homologue of the CD44 glycoprotein, is a lymph-specific receptor for hyaluronan. *J. Cell Biol.* **144**, 789–801 (1999).
18. Hadjantonakis, A.K., Macmaster, S. & Nagy, A. Embryonic stem cells and mice expressing different GFP variants for multiple non-invasive reporter usage within a single animal. *BMC Biotechnol.* **2**, 11 (2002).
19. Allen, C.D., Okada, T., Tang, H.L. & Cyster, J.G. Imaging of germinal center selection events during affinity maturation. *Science* **315**, 528–531 (2007).
20. Molina, H. *et al.* Markedly impaired humoral immune response in mice deficient in complement receptors 1 and 2. *Proc. Natl. Acad. Sci. USA* **93**, 3357–3361 (1996).
21. Cascalho, M., Ma, A., Lee, S., Masat, L. & Wabl, M. A quasi-monoclonal mouse. *Science* **272**, 1649–1652 (1996).
22. Miller, J.J. & Nossal, G.J.V. Antigens in Immunity VI. The phagocytic reticulum of lymph node follicles. *J. Exp. Med.* **120**, 1075–1095 (1964).
23. Mitchell, J. & Abbot, A. Ultrastructure of the antigen-retaining reticulum of lymph node follicles as shown by high-resolution autoradiography. *Nature* **208**, 500–502 (1965).
24. Bergtold, A., Desai, D.D., Gavhane, A. & Clynes, R. Cell surface recycling of internalized antigen permits dendritic cell priming of B cells. *Immunity* **23**, 503–514 (2005).
25. Veerman, A.J. & van Rooijen, N. Lymphocyte capping and lymphocyte migration as associated events in the *in vivo* antigen trapping process. An electron-microscopic autoradiographic study in the spleen of mice. *Cell Tissue Res.* **161**, 211–217 (1975).
26. Gray, D., Kumararatne, D.S., Lortan, J., Khan, M. & MacLennan, I.C. Relation of intrasplenic migration of marginal zone B cells to antigen localization on follicular dendritic cells. *Immunology* **52**, 659–669 (1984).
27. Groeneveld, P.H., Erich, T. & Kraal, G. The differential effects of bacterial lipopolysaccharide (LPS) on splenic non-lymphoid cells demonstrated by monoclonal antibodies. *Immunology* **58**, 285–290 (1986).
28. Ferguson, A.R., Youd, M.E. & Corley, R.B. Marginal zone B cells transport and deposit IgM-containing immune complexes onto follicular dendritic cells. *Int. Immunol.* **16**, 1411–1422 (2004).
29. Brown, J.C., De Jesus, D.G., Holborow, E.J. & Harris, G. Lymphocyte-mediated transport of aggregated human gamma-globulin into germinal centre areas of normal mouse spleen. *Nature* **228**, 367–369 (1970).
30. Heinen, E. *et al.* Transfer of immune complexes from lymphocytes to follicular dendritic cells. *Eur. J. Immunol.* **16**, 167–172 (1986).
31. Whipple, E.C., Shanahan, R.S., Ditto, A.H., Taylor, R.P. & Lindorfer, M.A. Analyses of the *in vivo* trafficking of stoichiometric doses of an anti-complement receptor 1/2 monoclonal antibody infused intravenously in mice. *J. Immunol.* **173**, 2297–2306 (2004).
32. Schwickert, T.A. *et al. In vivo* imaging of germinal centres reveals a dynamic open structure. *Nature* **446**, 83–87 (2007).
33. Boes, M. *et al.* Enhanced B-1 cell development, but impaired IgG antibody responses in mice deficient in secreted IgM. *J. Immunol.* **160**, 4776–4787 (1998).
34. Ehrenstein, M.R., O'Keefe, T.L., Davies, S.L. & Neuberger, M.S. Targeted gene disruption reveals a role for natural secretory IgM in the maturation of the primary immune response. *Proc. Natl. Acad. Sci. USA* **95**, 10089–10093 (1998).
35. Kraal, G. Cells in the marginal zone of the spleen. *Int. Rev. Cytol.* **132**, 31–73 (1992).
36. Mombaerts, P. *et al.* RAG-1-deficient mice have no mature B and T lymphocytes. *Cell* **68**, 869–877 (1992).
37. Phan, T.G. *et al.* B cell receptor-independent stimuli trigger immunoglobulin (Ig) class switch recombination and production of IgG autoantibodies by anergic self-reactive B cells. *J. Exp. Med.* **197**, 845–860 (2003).
38. Okada, T. *et al.* Antigen-engaged B cells undergo chemotaxis toward the T zone and form motile conjugates with helper T cells. *PLoS Biol.* **3**, e150 (2005).